Epidemics 37 (2021) 100491

Contents lists available at ScienceDirect

Epidemics

journal homepage: www.elsevier.com/locate/epidemics

Zika virus outbreak in Brazil under current and future climate

Tara Sadeghieh [a,b,c,*], Jan M. Sargeant [a,b], Amy L. Greer [a,b], Olaf Berke [a,b], Guillaume Dueymes [d], Philippe Gachon [d], Nicholas H. Ogden [c], Victoria Ng [c]

[a] Population Medicine, University of Guelph, Guelph, Ontario, Canada
[b] Centre for Public Health and Zoonoses, Ontario Veterinary College, University of Guelph, Guelph, Ontario, Canada
[c] Public Health Risk Sciences Division, National Microbiology Laboratory, Public Health Agency of Canada, Guelph, Ontario and St. Hyacinthe, Québec, Canada
[d] ESCER (Étude et Simulation du Climat à l'Échelle Régionale) Centre, Université du Québec à Montréal, Québec, Canada

ARTICLE INFO

Keywords:
Zika
Mosquito-borne disease
Climate change
Infectious disease model

ABSTRACT

Introduction: Zika virus (ZIKV) is primarily transmitted by*Aedes aegypti* and *Aedes albopictus* mosquitoes between humans and non-human primates. Climate change may enhance virus reproduction in *Aedes* spp. mosquito populations, resulting in intensified ZIKV outbreaks. The study objective was to explore how an outbreak similar to the 2016 ZIKV outbreak in Brazil might unfold with projected climate change.

Methods: A compartmental infectious disease model that included compartments for humans and mosquitoes was developed to fit the 2016 ZIKV outbreak data from Brazil using least squares optimization. To explore the impact of climate change, published polynomial relationships between temperature and temperature-sensitive mosquito population and virus transmission parameters (mosquito mortality, development rate, and ZIKV extrinsic incubation period) were used. Projections for future outbreaks were obtained by simulating transmission with effects of projected average monthly temperatures on temperature-sensitive model parameters at each of three future time periods: 2011–2040, 2041–2070, and 2071–2100. The projected future climate was obtained from an ensemble of regional climate models (RCMs) obtained from the Co-Ordinated Regional Downscaling Experiment (CORDEX) that used Representative Concentration Pathways (RCP) with two radiative forcing values, RCP4.5 and RCP8.5. A sensitivity analysis was performed to explore the impact of temperature-dependent parameters on the model outcomes.

Results: Climate change scenarios impacted the model outcomes, including the peak clinical case incidence, cumulative clinical case incidence, time to peak incidence, and the duration of the ZIKV outbreak. Comparing 2070–2100 to 2016, using RCP4.5, the peak incidence was 22,030 compared to 10,473; the time to epidemic peak was 12 compared to 9 weeks, and the outbreak duration was 52 compared to 41 weeks. Comparing 2070–2100 to 2016, using RCP8.5, the peak incidence was 21,786 compared to 10,473; the time to epidemic peak was 11 compared to 9 weeks, and the outbreak duration was 50 compared to 41weeks. The increases are due to optimal climate conditions for mosquitoes, with the mean temperature reaching 28 °C in the warmest months. Under a high emission scenario (RCP8.5), mean temperatures extend above optimal for mosquito survival in the warmest months.

Conclusion: Outbreaks of ZIKV in locations similar to Brazil are expected to be more intense with a warming climate. As climate change impacts are becoming increasingly apparent on human health, it is important to quantify the effect and use this knowledge to inform decisions on prevention and control strategies.

1. Introduction

Zika virus (ZIKV) is a flavivirus that belongs to the same genus as the viruses that cause dengue and yellow fever (Lowe et al., 2018; Weaver et al., 2016). These viruses are transmitted by mosquitoes, and in the case of ZIKV, mainly *Aedes aegypti*, but also *Ae. albopictus* (Lowe et al., 2018; Weaver et al., 2016). Both mosquito species are found in urban and suburban environments and share similar larval habitats (any water containers). *Aedes aegypti* are mostly found in tropical and subtropical locations (Lowe et al., 2018; Weaver et al., 2016). *Aedes albopictus* tolerates lower temperatures due to the diapause of overwintering eggs and is also found in temperate locations (Lowe et al., 2018; Weaver et al.,

* Corresponding author at: Population Medicine, University of Guelph, Guelph, Ontario, Canada.
E-mail address: tsadeghi@uoguelph.ca (T. Sadeghieh).

https://doi.org/10.1016/j.epidem.2021.100491
Received 7 October 2020; Received in revised form 6 August 2021; Accepted 17 August 2021
Available online 20 August 2021

2016). Zika virus can also be transmitted sexually, vertically from mother-to-child, and via blood transfusion; although, these modes of transmission are less common than mosquito-borne transmission (Lowe et al., 2018; Weaver et al., 2016). Generally, ZIKV disease has mild symptoms, including rash, fever, and headache. The disease is self-limiting and resolves in approximately one week; however, severe complications can occur, including Guillain-Barré syndrome and other possible neurological symptoms (Lowe et al., 2018; Weaver et al., 2016). Zika virus disease is especially serious for pregnant women, as it can impact the fetus, causing microcephaly and other congenital damage to the central nervous system (Lowe et al., 2018; Weaver et al., 2016). About 80 % of infected individuals are asymptomatic (Duffy et al., 2009; Lowe et al., 2018). Currently, there are no antiviral treatments, and there is no vaccine. Current ZIKV disease control methods include vector control by destroying vector habitats and insecticides use, and by personal protection from mosquito bites (Lowe et al., 2018; Weaver et al., 2016).

The ZIKV was first isolated in a rhesus monkey in the Zika forest of Uganda in 1947 (Wikan and Smith, 2016). Until this century regions endemic to ZIKV included Africa and Asia. Zika virus transmission has mainly occurred through sylvatic transmission cycles between non-human primate hosts and arboreal mosquitoes, similar to yellow fever in South America (Lowe et al., 2018; Weaver et al., 2016). In 2007, the first reported outbreak of ZIKV disease outside of Africa and Asia occurred in Yap State, part of the Federated States of Micronesia (Wikan and Smith, 2016). Since then, ZIKV infections have been reported in southeast Asia, French Polynesia, and the Americas (Wikan and Smith, 2016). The first reported case of ZIKV disease in Brazil occurred in Bahia on March 2015. The outbreak started in the east and spread westward (Lowe et al., 2018; Weaver et al., 2016). By 2016, ZIKV had spread to most states, except some remote states in the Amazon region, and the country's southernmost tip, where the climate is not favourable for the mosquito vectors (Lowe et al., 2018; Weaver et al., 2016). Zika virus disease became notifiable in Brazil on February 17, 2016 (Lowe et al., 2018; Weaver et al., 2016).

Human-induced global climate change is caused by increased emissions of greenhouse gases (GHG). Greenhouse gases are primarily from the combustion of fossil fuels and are regionally variable (Nema et al., 2012). Climate models predict future climates using projections for future concentrations and emissions of GHG and land-use change from four Representative Concentration Pathways (RCPs), which are defined by their total cumulative measure of anthropogenic GHG emissions by 2100 (van Vuuren et al., 2011a). The four RCP scenarios are: RCP2.6, which includes a scenario of strict mitigation of GHG emissions resulting in a very low forcing level; RCP4.5 and RCP6.0 are intermediate scenarios with medium stabilization scenarios; and RCP8.5 is a worst-case scenario, with a high baseline emission (van Vuuren et al., 2011b; IPCC, 2014). Currently, RCP2.6 is considered very unlikely, and RCP4.5 is becoming increasingly unlikely (van Vuuren et al., 2011b; IPCC, 2014).

In Brazil, anthropogenic climate change may cause an overall increase in temperature (Nema et al., 2012), although the rate of warming may vary across regions (IPCC Climate Change, 2013). With the changing climate, new regions in Brazil may become suitable for *Aedes.* spp. mosquitoes, such as at higher elevations, while others may become unsuitable, such as locations in the Amazon, which may become too hot for the survival of these mosquitoes (Lowe et al., 2018). Temperature has an impact on mosquito development and death rate, as well as the extrinsic incubation period (EIP), the time between mosquitoes getting infected to the time they can transmit the virus (Ciota and Keyel, 2019; Kamal et al., 2018; Wu et al., 2016). With increasing temperatures, the development rate is expected to accelerate as the mosquito completes its life stages faster; the death rate is expected to decrease, and then increase, as mosquito survival is reduced at higher temperatures; and the EIP is expected to decrease, as the higher temperature increases the replication rate of the virus in the mosquito (Lee et al., 2016; Marinho et al., 2016; Suparit et al., 2018; Tesla et al., 2018). The relationships between temperature and mosquito ecology are expected to change mosquito distribution throughout Brazil, and impact ZIKV transmission between humans and mosquitoes (Kamal et al., 2018). Locations in which ZIKV disease cases increases may also become sources of ZIKV geographic spread. Travellers returning from ZIKV-endemic areas, that have acquired infection and are viraemic on return (and therefore a source of infection for local vectors) have been detected in several countries, including France and Canada (Boggild et al., 2017; Maria et al., 2016; Wilder-Smith et al., 2018). Canada has reported 513 laboratory-confirmed cases as of June 2017, four of which originated from Brazil (Tataryn et al., 2018).

While analytic studies have been conducted to model the transmission and control of ZIKV (Buitrago Boret et al., 2017; Dantas et al., 2018; Fitzgibbon et al., 2017; Gao et al., 2016; Ogden et al., 2017; Suparit et al., 2018; Wang et al., 2017), there is currently no information on how ZIKV incidence in Brazil may change under future climate. It is expected that the number of cases will rise overall in Brazil due to the increase in temperature (Wu et al., 2016); however, the magnitude is unknown.

The objective of this study was to determine how the projected peak incidence, cumulative incidence, length of the outbreak, and time to peak incidence for a ZIKV disease outbreak similar to the 2016 outbreak may change, via the effects of future-projected climate on temperature-dependent parameters in the mosquito lifecycle and ZIKV transmission, under projections for future climate in time periods 2011–2040, 2041–2070, and 2071–2100, using the emissions scenarios in RCP4.5 and RCP8.5 to drive regional climate models.

2. Materials and methods

2.1. Data

We obtained ZIKV incidence data from the Health Information Platform for the Americas (Health Information Platform for the Americas (PLISA), n.d.). The climate data was obtained from the Co-Ordinated Regional Downscaling Experiment (CORDEX) (CORDEX; Giorgi et al., 2009) datasets. Parameter distributions for the compartment model were estimated based on literature (Table 1; Caminade et al., 2017; Duffy et al., 2009; Lee et al., 2016; Suparit et al., 2018; Zhang et al., 2017). Polynomial equations derived for the temperature-sensitive parameters used in the projection models were also based on literature (Table 3; Marinho et al., 2016; Tesla et al., 2018).

2.2. Model format

The 2016 ZIKV outbreak was used to the determine a baseline scenario and estimate the model outputs of an outbreak similar to the one in 2016 in three future time periods: 2011–2040, 2041–2070, 2071–2100. A schematic representation of a compartmental infectious disease model is presented in Fig. 1. The model is adapted from a previously described compartment model for chikungunya virus (Yakob and Clements, 2013). The model describes individuals' movement from susceptible (compartment S) to recovered humans (compartment R). When infectious mosquitoes (compartment Z) take a blood meal from humans (and may infect them), a proportion of the humans move from the susceptible (S) to exposed (E) compartments, representing humans that have been successfully infected during a blood meal. If susceptible mosquitoes (compartment X) bite infectious humans (compartments I and A), a proportion of the mosquitoes move to the exposed (Y) compartment, representing mosquitoes that have been successfully infected during a blood meal. The infectious human components included both symptomatic and asymptomatic compartments to account for the number of asymptomatic humans transmitting the virus but are not captured in surveillance data. It is assumed that all recovered humans have developed lifelong immunity, because although there is waning immunity, it

Table 1
Best fit parameters by week used in the ZIKV compartment model (T = temperature), where the transmission parameters were fitted to the 2016 ZIKV Brazil incidence data (Health Information Platform for the Americas (PLISA), n.d.).

Symbol	Name	Description	Best-fit value per week (distribution)	Source
β_1	Transmission rate (mosquito to human)	Rate at which infected mosquitos infects susceptible humans per week	2.65e-9	Fitted to 2016 Brazil ZIKV incidence
β_2	Transmission rate (human to mosquito)	Rate at which infected humans infect susceptible mosquitos per week	2.32e-8	Fitted to 2016 Brazil ZIKV incidence
ϕ	Proportion of symptomatic humans	Proportion of infected humans who develop symptoms	0.2	(Duffy et al., 2009; Zhang et al., 2017)
λ_1	Reciprocal of the intrinsic incubation period (human)	Rate of symptom onset after initial infection per week (human)	0.84 (scale = 0.78, shape = 3.5) (gamma)	(Lee et al., 2016; Suparit et al., 2018; Zhang et al., 2017)
λ_2	Reciprocal of the extrinsic incubation period (mosquito)	Rate at which mosquitoes are able to infect at the next blood meal after initial infection per week	0.74 (scale = 0.7, shape = 1.4) (gamma)	(Caminade et al., 2017; Lee et al., 2016; Suparit et al., 2018; Zhang et al., 2017)
γ	Duration of infectiousness (human)	Rate at which symptomatic and asymptomatic humans cease to be infectious per week	1.20 (scale = 1.0, shape = 2.3) (gamma)	(Caminade et al., 2017; Lee et al., 2016; Suparit et al., 2018; Zhang et al., 2017)
μ	Death rate (mosquito)	The rate at which mosquitos die per week	0.31 (min = 0.3, mean = 0.35, max = 0.9) (PERT)	(Lee et al., 2016; Suparit et al., 2018)
δ	Development rate (mosquito)	The rate at which mosquitoes develop from hatching to adult	0.60 (min = 0.5, mean = 0.58, max = 0.7) (PERT)	(Lee et al., 2016; Suparit et al., 2018)

may take several years to occur (Henderson et al., 2020). In order to keep the model simple, it is further assumed that the human population is closed throughout the outbreak (i.e., no births or deaths are included in the model). The mosquito compartment is open, and includes both the development rate of mosquitoes, as well as the death rate over one season. The vector being modelled is *Ae. aegypti*, the most likely vector of the 2016 ZIKV outbreak (Lowe et al., 2018). To further simplify the model, homogenous population mixing is assumed, where all humans and mosquitoes in Brazil are equally likely to acquire and transmit ZIKV. Transmission of ZIKV through sexual contact, blood transfusion, and mother-to-child was considered negligible in their contribution to the disease dynamics, and therefore, these routes of transmission were excluded from the model (Gao et al., 2016; Lowe et al., 2018). All parameters and initial conditions are described in Tables 1 and 2. The model was coded and developed in R (R Core Team, 2019, Vienna, Austria).

Table 2
Best fit initial conditions used in the non-climate dependent ZIKV compartment model, where the initial mosquito conditions were fitted to the 2016 ZIKV Brazil incidence data (Health Information Platform for the Americas (PLISA), n.d.).

Symbol	Name	Value	Notes/Source
N	Total human population	209,568,000	(United Nations Population Division, 2019)
S	Susceptible humans	209,538,028	Total human population minus remaining human compartments (N – E – I – A – R)
E	Exposed humans	6,868	fitted
I	Infectious humans (symptomatic)	2,525	First day of case count (Health Information Platform for the Americas (PLISA), n.d.)
A	Infectious humans (asymptomatic)	10,100	Estimated to be 80 % of the number of symptomatic humans (Duffy et al., 2009)
R	Recovered humans	10,478	Estimated (0.005 % of the population)
M	Total mosquito population	419,136,000	Estimated to be double the human population for each time period (Fitzgibbon et al., 2017; Wang et al., 2017)
X	Susceptible mosquitoes	419,128,869	Total mosquito population minus remaining mosquito components (M – Y – Z)
Y	Exposed mosquitoes	5,398	Fitted to 2016 Brazil ZIKV incidence
Z	Infectious mosquitoes	1,706	Fitted to 2016 Brazil ZIKV incidence

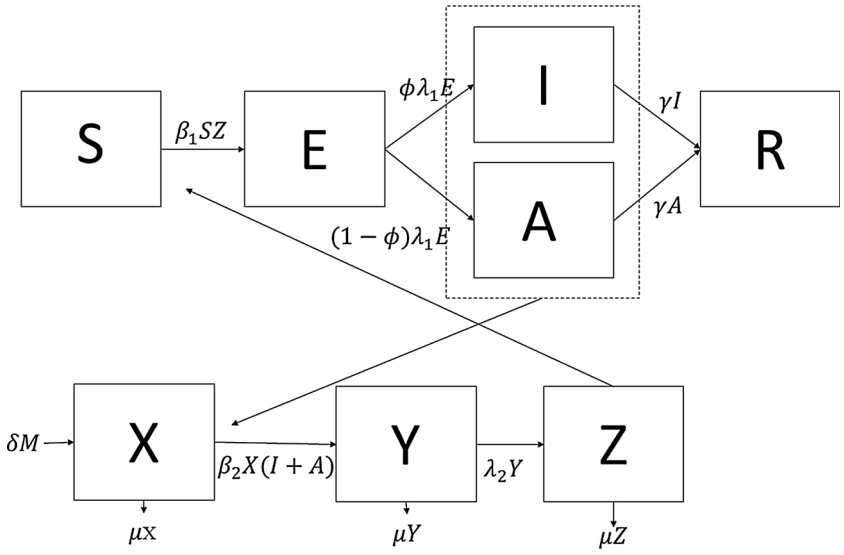

Fig. 1. The compartmental structure of the model, where S represents the number of susceptible humans, E are exposed humans, I are symptomatic infectious humans, A are asymptomatic infectious humans, R are recovered humans, X are susceptible mosquitoes, Y are exposed mosquitoes, and Z are infectious mosquitoes. The virus is transmitted from mosquitoes to humans with a probability of β_1 when infectious mosquitoes take a blood meal from susceptible humans, and the virus is transmitted from humans to mosquitoes with a probability of β_2 when susceptible mosquitoes take a blood meal from infectious humans (asymptomatic and symptomatic, as denoted by the dotted line). It was assumed that the mosquito population is double the human population (Fitzgibbon et al., 2017; Wang et al., 2017). Model parameters and initial conditions are described in Tables 1 and 2, respectively.

The dynamics of the ZIKV outbreak are described with the following ordinary differential equations, where the parameters and initial conditions are outlined in Tables 1 and 2 respectively:

$$\frac{dS}{dt} = -\beta_1 SZ$$

$$\frac{dE}{dt} = \beta_1 SZ - \lambda_1 E$$

$$\frac{dI}{dt} = \phi\lambda_1 E - \gamma I$$

$$\frac{dA}{dt} = (1-\phi)\lambda_1 E - \gamma A$$

$$\frac{dR}{dt} = \gamma(I + A)$$

$$\frac{dX}{dt} = \delta M - \beta_2 X(I + A) - \mu X$$

$$\frac{dY}{dt} = \beta_2 X(I + A) - \lambda_2 Y - \mu Y$$

$$\frac{dZ}{dt} = \lambda_2 Y - \mu Z$$

2.3. Optimization

We found the best fit transmission and initial mosquito parameters using least squares optimization. The projected ZIKV incidence was fit to the 2016 ZIKV incidence data in Brazil, as obtained from the Health Information Platform for the Americas (Health Information Platform for the Americas (PLISA), n.d.). Other parameters were allowed to vary within a set range and distribution (Table 1), to introduce variability into the model. The parameter distributions were identified using maximum likelihood estimation as implemented by the *fitdistplus* package in R (Delignette-Muller and Dutang, 2015). Ten thousand iterations were run using a box-constraint Broyden--Fletcher-Goldfarb-Shanno (L-BFGS-B) algorithm to find the global minimum with constraints on the parameters. The least squares optimization was conducted using R's *optim* function (R Core Team, 2019, Vienna, Austria).

2.4. Projecting model to future climate conditions

Climate data for the period when the 2016 outbreak occurred was not necessary as the climatic conditions under which it occurred are inherent in the data and thus assumed to represent the current climate period. Climate change and its potential impact on the ZIKV disease outbreaks were investigated using climate simulations from an ensemble of regional climate models (RCMs). These data were obtained from the CORDEX (Giorgi et al., 2009) datasets for the South America Domain with a horizontal resolution of 0.44° (SAM-44; CORDEX-SAM44, n.d.). An ensemble climate model was created for the monthly minimum and maximum temperatures (degree Celsius) for each RCP4.5 and RCP8.5 scenario for years 2011–2100 using nine individual models (S1). These two RCP scenarios were chosen as they represent middle- and worst-case scenario projections for climate change by 2100, and because CORDEX-SAM44 is only available for these two scenarios (CORDEX--SAM44, n.d.). In RCP4.5, the global climate models project a mean 2 °C increase in annual temperature globally, and a 1 °C warming for Brazil; while in RCP8.5, the models project a mean 4 °C increase in annual temperature globally, and a 2 °C warming for Brazil (IPCC, 2014). Projected mean monthly minimum and maximum daily temperatures were averaged, using a moving five-year average, to obtain projected monthly mean values, and then averaged across years at the monthly scale from the three 30-year time periods: 2011–2040, 2041–2070, and 2071–2100. To capture the temperature values for Brazil only, the grid values over Brazil were extracted using *R raster* (Hijmans, 2019) and *maptools* (Bivand and Lewin-Koh, 2019) packages. For RCP4.5, the average temperatures for the short-, medium-, and long-term time periods are 25.9 °C, 26.5 °C, and 26.9 °C respectively, and for RCP8.5, the average temperatures are 26.0 °C, 27.0 °C, and 28.3 °C (CORDEX--SAM44, n.d.). Polynomial equations were developed for three temperature-dependent mosquito parameters (EIP, death rate, and development rate) using field and laboratory data published in the literature (Table 3). The best-fit polynomial equations were chosen based on the R-squared values from the residuals between the fitted and observed case counts. The equations were then used with the best fit parameters from the optimized model for the 2016 outbreak to estimate the number of symptomatic infectious individuals over time for both RCP4.5 and RCP8.5. It was assumed that the outbreak was being introduced into a population where approximately 0.005 % of the individuals have immunity for each time period (Fig. 2).

The human population size was changed for each time period according to the projected average over each 30-year time period (221,537,000 for 2011–2040, 230,769,000 for 2041–2070, and 220,976,000 for 2071–2100) (United Nations Population Division, 2019).

2.5. Sensitivity analysis

A sensitivity analysis was conducted to determine which temperature-sensitive parameters (the mosquito parameters: death rate, development rate, and EIP) may most influence model outcomes. The analysis was conducted by determining how sensitive the model outcomes (peak incidence, number of weeks to peak, and outbreak duration) were to a 1 °C temperature change to three temperature-dependent mosquito variables. The parameter values were generated with the temperature set at 26 °C (which is the current average monthly temperature) and then generated at 27 °C, according to their relationship with temperature (Table 3). The model was, then, run with the new parameter values one-by-one for each parameter, while keeping the other parameters the same as the base model.

We also explored the relationship between temperature and the baseline (2016) compartment model. We accomplished this by inputting the average temperature of Brazil in 2016 (23.2 °C) into the polynomial equations for the temperature-sensitive parameters and using those values in the baseline model to see if the result of the model roughly matches the baseline model.

Finally, we explored the impact of population growth on model results rather than the temperature increase for the future time periods. We ran the model using: 1) the 2016 population and baseline parameters, 2) the long-term time period population and baseline parameters, 3) the 2016 population and long-term time period parameters and 4) the long-term time period population and long-term time period parameters. For each scenario, we determined the change in cumulative incidence when compared to the 2016 model results (scenario 1).

Table 3
Polynomial equations to describe the parameters' relationship to temperature (°C).

Parameter	Polynomial Equation	Source
Reciprocal of extrinsic incubation period	1/(1.213e3 - 1.463e2*T + 6.66*T^2 - 1.35e-1*T^3 + 1.026e-3*T^4)*7	(Tesla et al., 2018)
Death rate (mosquito)	1/(-67.7638 + 7.4757*T - 0.1503*T^2))*7	(Marinho et al., 2016)
Development rate (mosquito)	1/(120.73617 - 6.49746*T + 0.09554*T^2)*7	(Marinho et al., 2016)

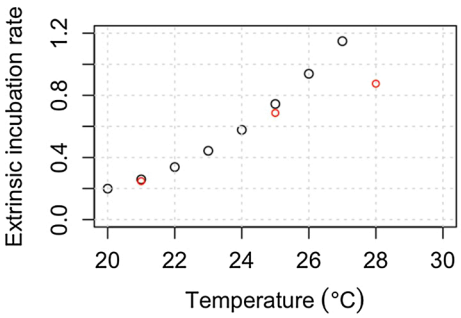

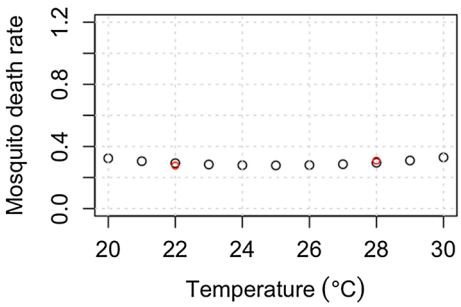

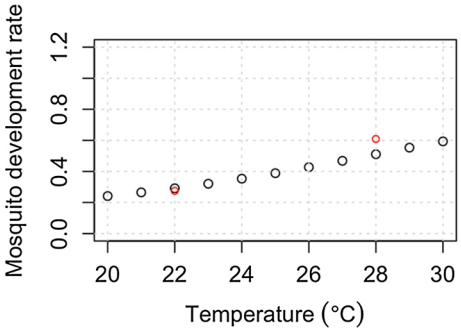

Fig. 2. Scatterplots showing the relationship of the three mosquito temperature-dependent parameters (EIP, lifespan, and development time) with temperature (°C). The red circles indicate the original field and laboratory data points. The EIP equation is based on data from Tesla et al., 2018, and the death and development rates of mosquitoes were based on Marinho et al., 2016. (For interpretation of the references to colour in this figure legend, the reader is referred to the web version of this article).

3. Results

3.1. Fitting the model to 2016 outbreak data

Model results for the number of symptomatic infectious humans are shown in Fig. 3 and indicate the best-minimized difference between the predicted and observed incidence in the 2016 Brazil ZIKV disease outbreak. The outbreak occurred from January to mid-October 2016, with the peak incidence of the outbreak occurring at week 9, and the duration of the outbreak was 41 weeks (Table 4). All best fit parameters and variables are shown in Tables 1 and 2, respectively. The model fits the maximum number of symptomatic infectious individuals well with a slight dip at the beginning. The fitted model outcome results are similar to the outbreak data (Table 4).

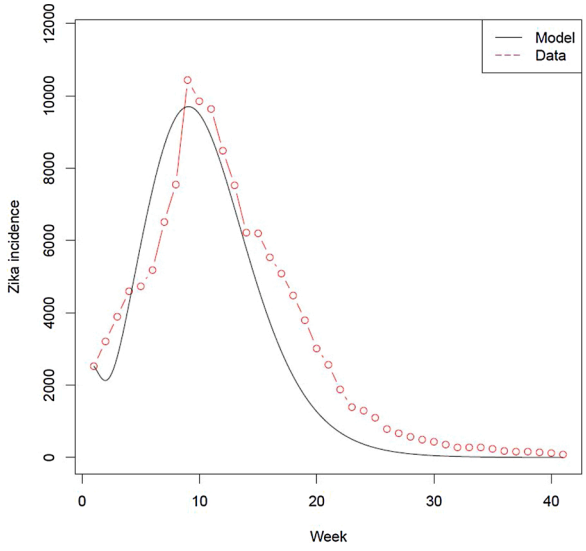

Fig. 3. Incidence of symptomatic ZIKV cases (black) over time in weeks according to the model output when the symptomatic infectious human compartment is fitted to the observed incidence of the 2016 ZIKV outbreak in Brazil (red dots and lines), from January to mid-October (Week 1 begins at January, week 10 at March, week 20 in mid-May, week 30 at the end of July, and week 41 at mid-October). (For interpretation of the references to colour in this figure legend, the reader is referred to the web version of this article).

3.2. Climate change impact on the simulated epidemic

The results of the model-based projections under the RCP4.5 climate change scenario are presented in Fig. 4. There was a 1.53-fold increase between the recent outbreak and the short-term time period (9116 cases), a 1.08-fold increase between short- and medium-term (1,753 cases), and a 1.02-fold increase between medium- and long-term (688 cases), indicating a non-linear pattern in the increase of cases. This pattern also occurred for the cumulative case counts (1.70-fold increase between the present outbreak and the short-term time period (130,417 cases), a 1.06-fold increase between short and medium-term (18,938 cases), and a 1.01-fold increase between medium and long term (6107 cases)). The number of weeks until the peak in incidence increased from week 10 to 12 for each future time period. The outbreak duration increased (41–53 weeks compared with the current time period, and then, for the long-term time period, reduced by one week (Table 4).

The results of the model-based projections under the RCP8.5 climate change scenario are presented in Fig. 5. There was a 1.55-fold increase in the peak number of cases between the present outbreak and the short-term time period (9,405 cases), a 1.11-fold increase between short- and medium-term (2,354 cases), and a 1.01-fold decrease between medium- and long-term time periods (446 cases), showing that the epidemic peak increased until the long-term time period, before decreasing. The same pattern occurred for the cumulative case counts (1.72-fold increase between the present outbreak and the short-term time period (133,715 cases), a 1.08-fold increase between short- and medium-term (23,109 cases), and a 1.06-fold decrease between medium- and long-term time periods (16,101 cases)). The number of weeks to peak incidence increased from the present time and mid-term time period (45 weeks to 53 weeks), before reducing between the mid-term time period and long-term time period to 52 weeks. The outbreak duration increased from the present time to the short-term time period

Table 4
Model results fit to the current outbreak (baseline scenario) and under future climates (RCP 4.5 and 8.5) for short-, medium-, and long-term time periods. In each column, blue indicates lower values, white indicates mid-range values, while red indicates higher values. The percentages below the values at the percent change when the outcome value is compared to the best fit model for the baseline outbreak. For references for the cumulative case count values, the estimated projected population of Brazil averaged for the short-, medium-, and long-term time periods are 221,537,000, 230,769,000, and 220,976,000 respectively (United Nations Population Division, 2019). (For interpretation of the references to colour in this table, the reader is referred to the web version of this article).

RCP Scenario	Time Periods	Peak symptomatic incidence	Cumulative incidence	Number of weeks to peak cases	Duration of outbreak (# of weeks)
Baseline	2016 ZIKV Outbreak	10,473	132,084	9	41
	Fitted results for outbreak	9,397	117,425	10	45
RCP4.5	2011 – 2040 (Short-term)	19,589 (108% increase)	262,501 (124% increase)	12 (20% increase)	53 (18% increase)
	2041 – 2070 (Medium-term)	21,342 (127% increase)	281,439 (140% increase)	12 (20% increase)	53 (18% increase)
	2071 – 2100 (Long-term)	22,030 (134% increase)	287,546 (145% increase)	12 (20% increase)	52 (16% increase)
RCP8.5	2011 – 2040 (Short-term)	19,878 (112% increase)	265,799 (126% increase)	12 (20% increase)	53 (18% increase)
	2041 – 2070 (Medium-term)	22,232 (137% increase)	288,908 (146% increase)	12 (20% increase)	52 (16% increase)
	2071 – 2100 (Long-term)	21,786 (132% increase)	272,807 (132% increase)	11 (10% increase)	50 (11% increase)

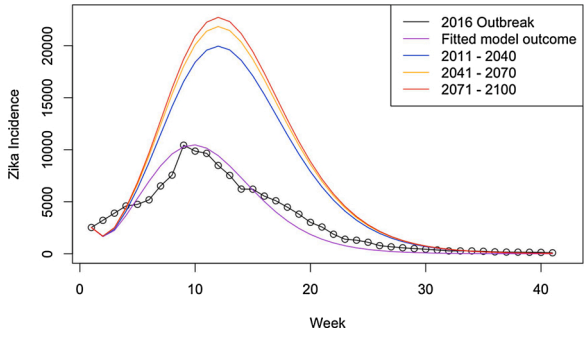

Fig. 4. Zika virus incidence (Compartment I) projected under RCP4.5, from 2011 to 2040 (blue), 2041 to 2070 (orange), and 2071 to 2100 (red), compared to weekly ZIKV incidence case count data in Brazil from the 2016 ZIKV outbreak (black dots and lines) and the model output fitted to the 2016 outbreak (purple). (For interpretation of the references to colour in this figure legend, the reader is referred to the web version of this article).

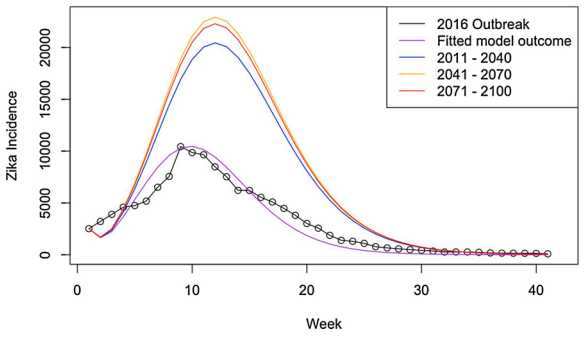

Fig. 5. Zika virus incidence (Compartment I) projected under RCP8.5, from 2011 to 2040 (blue), 2041 to 2070 (orange), and 2071 to 2100 (red), compared to weekly ZIKV case count data in Brazil from the 2016 ZIKV outbreak (black dots and lines), and the model output fitted to the 2016 outbreak (purple). (For interpretation of the references to colour in this figure legend, the reader is referred to the web version of this article).

(10 to 12 weeks) before decreasing to 11 weeks between the short-term time period and the long-term time period (Table 4).

3.3. Sensitivity analysis

The increase in the death rate of mosquitoes per week, caused by the increase in temperature, resulted in a reduction of the peak case count and outbreak duration. The increase in temperature also increased the development rate, which, in turn, increased the peak count and duration of the outbreak but decreased the number of weeks to the peak case count. The decreased EIP (increased rate) increased both the peak case count and the outbreak duration (Table 5).

When running the baseline model with the temperature data for 2016 for the temperature-sensitive parameters, we found the following: the peak symptomatic incidence was 9,632, the cumulative incidence was 133,755, the number of weeks to peak cases was 10 and the duration of the outbreak was 44. While the outcomes of the 2016 model with the inclusion of temperature caused slightly different values than our baseline model, they are still relatively similar (peak incidence = 9397, cumulative incidence = 117,425, number of weeks to peak incidence =

Table 5
Results of the sensitivity analysis for the death rate (μ), mosquito development rate (δ), and EIP (λ_2), where the parameters were calculated using their respective relationships to temperature (Table 3) at 26 °C and 27 °C. In each column, blue indicates lower values, white indicates mid-range values, while red indicates higher values. (For interpretation of the references to colour in this table, the reader is referred to the web version of this article).

Parameter	Temperature	Value per week	Peak incidence	Number of weeks to peak	Duration of outbreak (# of weeks)
μ	26°C	0.28	15,347	12	52
	27°C	0.29	13,315	12	50
δ	26°C	0.43	9,397	11	45
	27°C	0.47	11,182	10	46
$1/\lambda_2$	26°C	0.94	11,973	11	45
	27°C	1.15	12,249	11	46

10; duration of outbreak = 45; Table 4). This similarity suggests that our model captured the impact of temperature effectively.

The cumulative case incidence increased by 61 % in scenario 2 (population growth only), 92 % in scenario 3 (temperature increase only) and by 132 % in scenario 4 (both population growth and temperature increase) when compared to the cumulative incidence of the 2016 compartment model (baseline) (Table 6).

4. Discussion

The objective of this study was to determine how ZIKV outbreaks in subtropical regions may change under different future climate scenarios. In particular, we explored the effects of climate change on peak incidence, peak timing, final outbreak size, and outbreak duration. There have been several studies investigating ZIKV with and without the impacts of climate (Buitrago Boret et al., 2017; Dantas et al., 2018; Fitzgibbon et al., 2017; Gao et al., 2016; Ogden et al., 2017; Suparit et al., 2018; Tesla et al., 2018; Wang et al., 2017). This study contributes to research on ZIKV by investigating how ZIKV epidemiology may change under future climate scenarios in Brazil. We found that, first, there was a non-linear relationship between projected climate change and ZIKV transmission; second, human cases of ZIKV increased as temperature increased in the short- and medium-term time periods, but this increase was slightly lower in the longer-term time period; and finally, the outbreak length decreased as temperature increased indicating transmission occurs faster within the population with increasing temperature.

Our findings showed a general increase in human cases of ZIKV with increasing temperature under future climate conditions. This pattern has previously been predicted for dengue, where there was a sharp increase in projected dengue transmission before 2050, followed by a smaller increase after 2050 (Åström et al., 2012). The pattern we observed was due to a combination of the rapid increase in temperature over the short- and medium-term time period (anticipated to be 0.4 °C under RCP4.5) compared to a slower increase in temperature over the long-term time period (0.6 °C under RCP4.5) (CORDEX-SAM44, n.d.) in combination with the non-linear relationships between temperature and temperature-dependent parameters, EIP, development and death rates (Marinho et al., 2016; Tesla et al., 2018). We found that, for RCP8.5, the maximum number of symptomatic infectious individuals was higher in the medium-term time period versus the long-time period, which is different from RCP4.5. This trend is because the projected average temperature between 2071–2100 under RCP8.5 is often greater than 28 °C. A temperature of 28 °C is the threshold at which the development rate of *Aedes* mosquitoes are counterbalanced by the effects of the temperature on the death rate, causing the mosquito population size to contract (Marinho et al., 2016; Rogers, 2015; Tesla et al., 2018).

Our findings suggest that the duration of an outbreak will decrease as temperature increases. The shorter duration is due to a shorter EIP and quicker development rate, thereby allowing the mosquitoes to spread the virus faster. This trend was observed in the long-term time period for RCP4.5 and the medium-term time period for RCP8.5, which also have higher outbreak size than the previous time periods. Previous studies have also suggested that climate change may result in an increased incidence of mosquito-borne diseases, including West Nile virus (Paz, 2015) and dengue (Ebi and Nealon, 2016; Lee et al., 2018; Patz et al., 1998) due to increasing temperatures, which corresponds with our findings. The shorter outbreak may also indicate a less intense outbreak overall, as observed in the long-term time period for RCP8.5, which projected a smaller outbreak size than the previous time period due to the decrease in mosquito abundance. This reduction in outbreak duration has also been projected for subtropical and tropical regions where long-term climate change is anticipated to be above the optimal climatic suitability for mosquito development and viral replication, such as dengue in Australia (Williams et al., 2016).

The sensitivity analysis showed that, with increased temperature, the increased death rate in mosquitoes decreased the peak incidence in humans, while the increased development rate and EIP increased the peak incidence. The outbreak duration followed the same pattern. These findings are consistent with a previous study that found that mosquitoes' mortality rate increased with increasing temperature, while EIP decreased with increasing temperature (Lee et al., 2016). Of the three temperature-dependent variables, death and development rates were most sensitive to temperature increases; therefore, much of the increase in cases may be explained by the impact of temperature on the lifecycle of mosquitoes rather than the impact of temperature on virus replication within mosquitoes. A modelling study conducted on dengue in China also found the mosquito lifecycle to be important in explaining dengue

Table 6
Exploring the impact of population growth versus temperature on the cumulative incidence compared to the results of the baseline model.

Scenario	Cumulative incidence	Percent increase (compared to baseline scenario)
1: Baseline (2016 model results)	117,425	NA
2: 2016 model with the human population used for the long-term time period (N = 220,976,000)	189,054	61 %
3: 2016 model with temperature-sensitive parameter values used for the long-term time period (Table 3)	225,634	92 %
4: Long-term time period model results	272,807	132 %

outbreaks, as infected mosquitoes must survive the length of the EIP before they can spread dengue (Li et al., 2018).

Our sensitivity analysis also showed that, while both population growth and temperature increase resulted in an increase of cases, when considering solely one or the other, temperature increase had a greater impact on the increase in cumulative incidence. An increase in temperature impacts case incidence due to the effect of temperature on mosquito parameters. The development rate is expected to quicken, the death rate to slow and then quick, and the EIP to decrease (Lee et al., 2016; Marinho et al., 2016; Suparit et al., 2018; Tesla et al., 2018). With these changes, mosquitoes are expected to polifertate quicker and be more likely to live through the EIP, thus being more likely to transmit ZIKV to humans. An increase in population increases the number of susceptible humans (Lee et al., 2016). The relationship between population, climate and disease is complex. Population growth can impact the severity of climate change, and other factors such as land use and land changes would allow greater contact between mosquitoes and humans (Lambin et al., 2010; Macdonald and Mordecai, 2019); Satterthwaite, 2009). In our model, for simplicity we assume the only changes in the future scenarios are climate change and population growth. From out sensitivity analysis, it appears that climate change may have a greater influence on Zika incidence than population growth if the only impact of population growth is the increase of susceptible individuals.

Our study is not without limitations. This model employed some simplifying assumptions and did not capture Brazil's population or geographic heterogeneity, which can influence parameters in the model (Perkins et al., 2016; Carlson et al., 2016). Our fitted transmission rates were small, possibly because the total number of reported cases of ZIKV (132,084) was small compared to the overall number of cases that occurred and to the population of Brazil (209,568,000), resulting in a small overall attack rate (0.0006 %). The ZIKV incidence data were not available at the county-level, and the model was therefore fitted at the national level. Model calibration was conducted using one outbreak year (2016), and thus it is possible that model results are biased, and could be underreporting ZIKV incidence in Brazil (Morrison and Cunha, 2020). Despite the simplifying assumptions, the model fit the outbreak data well. The model also did not take into account changes that may occur over time in Brazil, such as deforestation and other land changes, which have an impact on mosquito-borne diseases by introducing more cases as contact between human and mosquito populations increases (Chaves et al., 2018; Lambin et al., 2010; Macdonald and Mordecai, 2019). Previous studies have noted that precipitation impacts mosquito-borne diseases by creating or destroying potential egg-laying locations (Alto and Juliano, 2001; Lega et al., 2017). Precipitation in Brazil is expected to decrease under future climate conditions (IPCC, 2014). The increased temperatures and decreased precipitation are expected to reduce *Aedes* populations (Alto and Juliano, 2001; Ryan et al., 2018), especially *Ae. albopictus* across all of Brazil, and *Ae. aegypti* mainly in the Amazon basin (Ryan et al., 2018). Thus, this study may overestimate ZIKV incidence as precipitation decreases over time in combination with temperature increase. There are uncertainties in the precipitation signal under climate change over tropical areas, especially for extreme rainfall over continental areas (IPCC Climate Change, 2013; Kent et al., 2015). Further research is required using precipitation signals from CORDEX runs. The univariate sensitivity analysis performed did is not as robust as multivariate techniques; however, the purpose of the analysis was to explore temperature-sensitive parameter impacts on model outcomes, and not as an uncertainty analysis. Despite our model's simplicity, it can be used as a framework for more complex models.

Our model did not explore other forms of ZIKV transmission, such as sexual transmission, blood transfusions, or vertical transmission. These modes of transmission contribute only a small proportion of ZIKV transmissions and have a negligible impact on the outcome (Gao et al., 2016; Lowe et al., 2018). A modelling study estimated 3.04 % of ZIKV cases are transmitted via sexual transmission, and that this is not a viable transmission route to sustain an outbreak (Gao et al., 2016). Last, there are inherent uncertainties in climate models (Soden et al., 2018; Wootten et al., 2017); however, we used an ensemble of models to reduce the impact of biases and uncertainty in individual climate models.

5. Conclusion

Climate change is anticipated to have an impact on human health in general and on mosquito-borne diseases. Climate change is expected to increase Brazil's overall temperature, thereby increasing the mosquito population with potential consequences to humans. This study explored and quantified the impact of increasing temperature due to climate change on a ZIKV outbreak similar to Brazil in 2016. Findings from this study show that the impact of temperature will vary across different time periods depending on the climate change trajectory in Brazil. This trend is anticipated to have a subsequent impact on other countries that may observe an increase in imported cases of mosquito-borne diseases due to climate change. Further research should focus on more regionalized models, such as specific regions in Brazil that vary from one another, both at the present and future climate, and include other predictors, such as land-use changes and regional changes in precipitation and climate variability. Our study highlights the need for advanced preparation, mitigation, and prevention of future outbreaks of mosquito-borne diseases compounded by climate change.

Author contributions

Tara Sadeghieh: Conceptualization, data curation, formal analysis, investigation, methodology, software, validation, visualization, writing – original draft, writing – review and editing.

Jan M. Sargeant: Supervision, validation, writing – review and editing.

Amy L. Greer: Supervision, methodology, validation, writing – review and editing.

Olaf Berke: Supervision, validation, writing – review and editing.

Guillaume Dueymes: Data curation, investigation, software, writing – review and editing.

Philippe Gachon: Data curation, investigation, software, writing – review and editing.

Nicholas H. Ogden: Supervision, methodology, validation, writing – review and editing.

Victoria Ng: Conceptualization, methodology, supervision, validation, writing – review and editing.

Involvement of funding source

The PhD candidate's (TS) stipend was provided by the Public Health Agency of Canada (PHAC). VN is TS's co-supervisor and an employee of PHAC.

Declaration of Competing Interest

The authors report no declarations of interest. This research required no ethics approval as it only used publicly available unidentifiable data.

Appendix A. Supplementary data

Supplementary material related to this article can be found, in the online version, at doi:https://doi.org/10.1016/j.epidem.2021.100491.

References

Alto, B.W., Juliano, S.A., 2001. Precipitation and temperature effects on populations of *Aedes albopictus* (Diptera: Culicidae): implications for range expansion. J. Med. Entomol. 38, 646–656. https://doi.org/10.1603/0022-2585-38.5.646.

Åström, C., Rocklöv, J., Hales, S., Béguin, A., Louis, V., Sauerborn, R., 2012. Potential distribution of dengue fever under scenarios of climate change and economic development. Ecohealth 9, 448–454. https://doi.org/10.1007/s10393-012-0808-0.
Bivand, R., Lewin-Koh, N., 2019. Maptools: Tools for Handling Spatial Objects.
Boggild, A.K., Geduld, J., Libman, M., Yansouni, C.P., McCarthy, A.E., Hajek, J., Ghesquiere, W., Mirzanejad, Y., Vincelette, J., Kuhn, S., Plourde, P.J., Chakrabarti, S., Freedman, D.O., Kain, K.C., 2017. Surveillance report of Zika virus among Canadian travellers returning from the Americas. CMAJ 189, E334–E340. https://doi.org/10.1503/cmaj.161241.
Buitrago Boret, S.E., Escalante, R., Villasana, M., 2017. Mathematical modelling of zika virus in Brazil. J. LATEX Templates.
Caminade, C., Turner, J., Metelmann, S., Hesson, J.C., Blagrove, M.S., Solomon, T., Morse, A.P., Baylis, M., 2017. Global risk model for vector-borne transmission of Zika virus reveals the role of El Nino 2015.[Erratum appears in Proc Natl Acad Sci U S A. 2017 Feb 14;114(7):E1301-E1302; PMID: 28137863]. Proc. Natl. Acad. Sci. U. S. A. 114, 119–124. https://doi.org/10.1073/pnas.1614303114.
Carlson, C.J., Dougherty, E.R., Getz, W., 2016. An ecological assessment of the pandemic threat of Zika virus. PLoS Negl. Trop. Dis. 10, e0004968 https://doi.org/10.1371/journal.pntd.0004968.
Chaves, L.S.M., Conn, J.E., López, R.V.M., Sallum, M.A.M., 2018. Abundance of impacted forest patches less than 5 km2 is a key driver of the incidence of malaria in Amazonian Brazil. Sci. Rep. 8, 1–11. https://doi.org/10.1038/s41598-018-25344-5.
Ciota, A.T., Keyel, A.C., 2019. The role of temperature in transmission of zoonotic arboviruses. Viruses 11 (11), 1013. https://doi.org/10.3390/v11111013.
CORDEX-SAM44, n.d. CORDEX [WWW Document]. URL https://esg-dn1.nsc.liu.se/search/cordex/ (accessed 6.20.19).
Dantas, E., Tosin, M., Cunha, A., 2018. Calibration of a SEIR–SEI epidemic model to describe the Zika virus outbreak in Brazil. Appl. Math. Comput. 338, 249–259. https://doi.org/10.1016/j.amc.2018.06.024.
Delignette-Muller, M.L., Dutang, C., 2015. Fitdistrplus: an R package for fitting distributions. J. Stat. Softw. 64 (4), 1–34. http://www.jstatsoft.org/v64/i04/.
Duffy, M.R., Chen, T.-H., Hancock, W.T., Powers, A.M., Kool, J.L., Lanciotti, R.S., Pretrick, M., Marfel, M., Holzbauer, S., Dubray, C., Guillaumot, L., Griggs, A., Bel, M., Lambert, A.J., Laven, J., Kosoy, O., Panella, A., Biggerstaff, B.J., Fischer, M., Hayes, E.B., 2009. Zika virus outbreak on Yap Island, Federated States of Micronesia. N. Engl. J. Med. 360, 2536–2543. https://doi.org/10.1056/NEJMoa0805715.
Ebi, K.L., Nealon, J., 2016. Dengue in a changing climate. Environ. Res. 151, 115–123. https://doi.org/10.1016/j.envres.2016.07.026.
Fitzgibbon, W.E., Morgan, J.J., Webb, G.F., 2017. An outbreak vector-host epidemic model with spatial structure: the 2015-2016 Zika outbreak in Rio De Janeiro. Theor. Biol. Med. Model. 14, 7. https://doi.org/10.1186/s12976-017-0051-z.
Gao, D., Lou, Y., He, D., Porco, T.C., Kuang, Y., Chowell, G., Ruan, S., 2016. Prevention and control of Zika as a mosquito-borne and sexually transmitted disease: a mathematical modeling analysis. Sci. Rep. 6 https://doi.org/10.1038/srep28070.
Giorgi, F., Jones, C., Asrar, G.R., 2009. Addressing climate information needs at the regional level: the CORDEX framework. World Meteorol. Organiz. (WMO) Bull. 58 (3).
Health Information Platform for the Americas (PLISA), n.d. Zika indicators [WWW Document]. URL http://www.paho.org/data/index.php/en/?option=com_content&view=article&id=524&Itemid= (accessed 2.10.19).
Henderson, A.D., Aubry, M., Kama, M., Vanhomwegen, J., Teissier, A., Mariteragi-Helle, T., Paoaafaite, T., Teissier, Y., Manuguerra, J., Edmunds, J., Whitworth, J., Watson, C.H., Lau, C.L., Cao-Lormeau, V., Kucharski, A.J., 2020. Zika seroprevalence declines and neutralizing antibodies wane in adults following outbreaks in French Polynesia and Fiji. eLife 9, e48460.
Hijmans, R.J., 2019. raster: Geographic Data Analysis and Modeling.
IPCC, 2014. Climate Change, 2014: Synthesis Report.
IPCC Climate Change, 2013. In: Stocker, T.F., et al. (Eds.), The Physical Science Basis. Cambridge Univ. Press, Cambridge.
Kamal, M., Kenawy, M.A., Rady, M.H., Khaled, A.S., Samy, A.M., 2018. Mapping the global potential distributions of two arboviral vectors Aedes aegypti and Ae. Albopictus under changing climate. PLoS One 13. https://doi.org/10.1371/journal.pone.0210122.
Kent, C., Chadwick, R., Rowell, D.P., 2015. Understanding uncertainties in future projections of seasonal tropical precipitation. J. Climate 28, 4390–4413. https://doi.org/10.1175/JCLI-D-14-00613.1.
Lambin, E.F., Tran, A., Vanwambeke, S.O., Linard, C., Soti, V., 2010. Pathogenic landscapes: interactions between land, people, disease vectors, and their animal hosts. Int. J. Health Geogr. 9, 54.
Lee, E.K., Liu, Y., Pietz, F.H., 2016. A compartmental model for Zika virus with dynamic human and vector populations. AMIA … Annu. Symp. Proceedings. AMIA Symp. 743–752.
Lee, H., Kim, J.E., Lee, S., Lee, C.H., 2018. Potential effects of climate change on dengue transmission dynamics in Korea. PLoS One 13. https://doi.org/10.1371/journal.pone.0199205.
Lega, J., Brown, H.E., Barrera, R., 2017. Aedes aegypti (Diptera: Culicidae) abundance model improved with relative humidity and precipitation-driven egg hatching. J. Med. Entomol. 54, 1375–1384. https://doi.org/10.1093/jme/tjx077.
Li, Chenlu, Lu, Yongmei, Liu, Jianing, Wu, Xiaoxu, 2018. Climate change and dengue fever transmission in China: Evidences and challenges. Sci. Total Environ. 622-623, 493–501. https://doi.org/10.1016/j.scitotenv.2017.11.326.
Lowe, R., Barcellos, C., Brasil, P., Cruz, O.G., Honório, N.A., Kuper, H., Carvalho, M.S., 2018. The zika virus epidemic in brazil: from discovery to future implications. Int. J. Environ. Res. Public Health 15. https://doi.org/10.3390/ijerph15010096.
Macdonald, A.J., Mordecai, E.A., 2019. Amazon deforestation drives malaria transmission, and malaria burden reduces forest clearing. Proc. Natl. Acad. Sci. U. S. A. 116, 44.
Maria, A.T., Maquart, M., Makinson, A., Flusin, O., Segondy, M., Leparc-Goffart, I., Le Moing, V., Foulongne, V., 2016. Zika virus infections in three travellers returning from South America and the Caribbean respectively, to Montpellier, France, December 2015 to January 2016. Eurosurveillance 21, 30131. https://doi.org/10.2807/1560-7917.ES.2016.21.6.30131.
Marinho, R.A., Beserra, E.B., Bezerra-Gusmão, M.A., Porto, Vde S., Olinda, R.A., dos Santos, C.A.C., 2016. Effects of temperature on the life cycle, expansion, and dispersion of *Aedes aegypti* (Diptera: Culicidae) in three cities in Paraiba, Brazil. J. Vector Ecol. 41, 1–10. https://doi.org/10.1111/jvec.12187.
Morrison, R.E., Cunha, A., 2020. Emdedded model discrepancy: a case study of Zika modeling. Chaos 30.
Nema, P., Nema, S., Roy, P., 2012. An overview of global climate changing in current scenario and mitigation action. Renew. Sustain. Energy Rev. 16 (4), 2329–2336. https://doi.org/10.1016/j.rser.2012.01.044.
Ogden, N.H., Fazil, A., Safronetz, D., Drebot, M.A., Wallace, J., Rees, E.E., Decock, K., Ng, V., 2017. Risk of travel-related cases of Zika virus infection is predicted by transmission intensity in outbreak-affected countries. Parasit. Vectors 10, 41. https://doi.org/10.1186/s13071-017-1977-z.
Patz, J.A., Martens, W.J.M., Focks, D.A., Jetten, T.H., 1998. Dengue fever epidemic potential as projected by general circulation models of global climate change. Environ. Health Perspect. 106, 147–153. https://doi.org/10.1289/ehp.98106147.
Paz, S., 2015. Climate change impacts on West Nile virus transmission in a global context. Philos. Trans. R. Soc. B Biol. Sci. 370, 1–11. https://doi.org/10.1098/rstb.2013.0561.
Perkins, T., Siraj, A.S., Ruktanonchai, C.W., Kraemer, M.U.G., Tatem, A.J., 2016. Model-based projections of Zika virus infections in childbearing women in the Americas. Nat. Microbiol. 1 https://doi.org/10.1038/nmicrobiol.2016.126.
Rogers, D.J., 2015. Dengue: recent past and future threats. Philos. Trans. R. Soc. B Biol. Sci. 370, 1–18. https://doi.org/10.1098/rstb.2013.0562.
Ryan, S.J., Carlson, C.J., Mordecai, E.A., Johnson, L.R., 2018. Global expansion and redistribution of Aedes-borne virus transmission risk with climate change. PLoS Negl. Trop. Dis. 13 https://doi.org/10.1371/journal.pntd.0007213.
Satterthwaite, D., 2009. The implications of population growth and urbanization for climate change. Environ. Urban. 21 https://doi.org/10.1177/0956247809344361.
Soden, B.J., Collins, W.D., Feldman, D.R., 2018. Reducing uncertainties in climate models. Science (80-.) 361.
Suparit, P., Wiratsudakul, A., Modchang, C., 2018. A mathematical model for Zika virus transmission dynamics with a time-dependent mosquito biting rate. Theor. Biol. Med. Model. 15, 11. https://doi.org/10.1186/s12976-018-0083-z.
Tataryn, J., Vrbova, L., Drebot, M., Wood, H., Payne, E., Connors, S., Geduld, J., German, M., Khan, K., Buck, P., 2018. Travel-related Zika virus cases in Canada: October 2015–June 2017. Canada Commun. Dis. Rep. 44, 18–26. https://doi.org/10.14745/ccdr.v44i01a05.
Tesla, B., Demakovsky, L.R., Mordecai, E.A., Ryan, S.J., Bonds, M.H., Ngonghala, C.N., Brindley, M.A., Murdock, C.C., 2018. Temperature drives Zika virus transmission: evidence from empirical and mathematical models. Proc. R. Soc. B Biol. Sci. 285 https://doi.org/10.1098/rspb.2018.0795.
United Nations Population Division, 2019. World Population Prospects: The 2019 Revision [WWW Document]. URL http://data.un.org/Data.aspx?q=population+brazil+&d=PopDiv&f=variableID%3A12%3BcrID%3A76 (accessed 4.10.19).
van Vuuren, D.P., Edmonds, J., Kainuma, M., Riahi, K., Thomson, A., Hibbard, K., Hurtt, G.C., Kram, T., Krey, V., Lamarque, J.F., Masui, T., Meinshausen, M., Nakicenovic, N., Smith, S.J., Rose, S.K., 2011a. The representative concentration pathways: an overview. Clim. Change 109, 5–31. https://doi.org/10.1007/s10584-011-0148-z.
van Vuuren, D.P., Edmonds, J.A., Kainuma, M., Riahi, K., Weyant, J., 2011b. A special issue on the RCPs. Clim. Change 109, 1–4. https://doi.org/10.1007/s10584-011-0157-y.
Wang, L., Zhao, H., Muniz Oliva, S., Zhu, H., 2017. Modeling the transmission and control of Zika in Brazil. Nature 7, 7721. https://doi.org/10.1038/s41598-017-07264-y.
Weaver, S.C., Costa, F., Garcia-Blanco, M.A., Ko, A.I., Ribeiro, G.S., Saade, G., Shi, P.Y., Vasilakis, N., 2016. Zika virus: history, emergence, biology, and prospects for control. Antiviral Res. https://doi.org/10.1016/j.antiviral.2016.03.010.
Wikan, N., Smith, D.R., 2016. Zika virus: history of a newly emerging arbovirus. Lancet Infect. Dis. 16 (7), 119–126. https://doi.org/10.1016/S1473-3099(16)30010-X.
Wilder-Smith, A., Chang, C.R., Leong, W.Y., 2018. Zika in travellers 1947–2017: a systematic review. J. Travel Med. 25.
Williams, C.R., Mincham, G., Faddy, H., Viennet, E., Ritchie, S.A., Harley, D., 2016. Projections of increased and decreased dengue incidence under climate change. Epidemiol. Infect. 144, 3091–3100. https://doi.org/10.1017/S095026881600162X.
Wootten, A., Terando, A., Reich, B.J., Boyles, R.P., Semazzi, F., 2017. Characterizing sources of uncertainty from global climate models and downscaling techniques. J. Appl. Meteorol. Climatol. 56, 3245–3262. https://doi.org/10.1175/JAMC-D-17-0087.1.
Wu, X., Lu, Y., Zhou, S., Chen, L., Xu, B., 2016. Impact of climate change on human infectious diseases: empirical evidence and human adaptation. Environ. Int. 86, 14–23. https://doi.org/10.1016/j.envint.2015.09.007.
Yakob, L., Clements, A.C.A., 2013. A mathematical model of chikungunya dynamics and control: the major epidemic on Réunion Island. PLoS One 8, e57448. https://doi.org/10.1371/journal.pone.0057448.
Zhang, Q., Sun, K., Chinazzi, M., Piontti, A.P.Y., Dean, N.E., Rojas, Di.P., Merler, S., Mistry, Di., Poletti, P., Rossi, L., Bray, M., Halloran, M.E., Longini, I.M.,

Vespignani, A., 2017. Spread of Zika virus in the Americas. Proc. Natl. Acad. Sci. U. S. A. 114, E4334–E4343. https://doi.org/10.1073/pnas.1620161114.